Geothermometry, geobarometry and the Al₂SiO₅ triple point at Mt. Moosilauke, New Hampshire

K. V. Hodges[1] and F. S. Spear

Center for Geoalchemy
Department of Earth and Planetary Sciences
Massachusetts Institute of Technology, Cambridge, Massachusetts 02139

Abstract

Near Mt. Moosilauke, New Hampshire, the distribution of aluminum silicate minerals in pelitic schists constrains pressure and temperature conditions during the Acadian orogeny to have been approximately those of the Al_2SiO_5 invariant point, thus providing an excellent opportunity to evaluate the internal consistency of a variety of published geothermometers and geobarometers with the Al_2SiO_5 invariant point of Holdaway (1971). Four fluid-independent equilibria, garnet–biotite Fe–Mg exchange (Ferry and Spear, 1978), garnet–plagioclase–Al₂SiO₅–quartz (Ghent *et al.*, 1979) and garnet–plagioclase–quartz–biotite–muscovite (Fe and Mg end members, Ghent and Stout, 1981), yield P–T estimates consistent with the experimental Al_2SiO_5 triple point of Holdaway (1971). Two fluid-dependent equilibria, garnet–staurolite–quartz–Al₂SiO₅–H₂O (Hutcheon, 1979) and plagioclase–muscovite–Al₂SiO₅–quartz–H₂O (Cheney and Guidotti, 1979), applied assuming $P(H_2O)$ near P_{total}, yield internally consistent but unrealistically high temperatures, suggesting $P(H_2O) \ll P_{total}$.

Despite good agreement with Holdaway's triple point, the Ferry–Spear garnet–biotite geothermometer and the Ghent *et al.* garnet–plagioclase–aluminosilicate–quartz geobarometer adopt conflicting garnet solution models. We present alternative calibrations that use a consistent set of solution models. Activity coefficients and Margules parameters for plagioclase and garnet solid solutions have been constrained by assuming triple point P–T conditions for the Moosilauke samples and solving for the values of interest. Our data are consistent with the conclusions that: (1) only pyrope–grossular mixing in the quaternary garnet system is significantly non-ideal; and (2) the activity coefficient for the anorthite component in plagioclase is approximately 2 at triple point P–T conditions.

Introduction

The usefulness of a given geothermometer or geobarometer in determining "peak" metamorphic conditions for natural assemblages depends on: (1) the inherent accuracy of the calibration used, (2) whether or not the effects of additional components have been accurately accounted for, (3) the degree of equilibration at "peak" metamorphic conditions and (4) whether or not the phases involved have reequilibrated during cooling and uplift. Whereas inherent accuracy is difficult, if not impossible to evaluate, calibrated mineral equlibria can be tested for consistency with experimentally-determined mineral stabilities. Toward this end, we have applied six widely used geothermometers/geobarome-

ters to pelitic schists of the Mt. Moosilauke region, New Hampshire, where the distribution of Al_2SiO_5 polymorphs tightly constrains the pressure and temperature conditions during peak metamorphism to be very near those of the aluminum silicate triple point.

As they originally appeared in the literature, many of the calibrations used in this exercise are inconsistent with regard to the solution models assumed for pure phases. In the final sections of this paper, we present more internally consistent calibrations for two of the most useful equilibria: the garnet–biotite geothermometer and the garnet–plagioclase–aluminum silicate–quartz geobarometer.

Geologic setting of the Mt. Moosilauke area

Thompson and Norton (1968) suggested that a continuous, roughly N–S line could be drawn

across a map of New England such that all occurrences of andalusite produced during Acadian regional metamorphism lie to its east (Fig. 1). This line was considered to be the trace of "a fossil isobaric surface corresponding to the pressure of the kyanite–andalusite–sillimanite triple point". According to Thompson and Norton's (1968) metamorphic map of New England, the kyanite = sillimanite and andalusite = sillimanite isograds should intersect the "triple point isobar" in the vicinity of Mt. Moosilauke, New Hampshire. Unfortunately, outcrops of pelitic schists are discontinuous in this area and do not allow the location of this intersection with precision. However, in an exhaustive study of aluminum silicate distribution in this area, Rumble (1973) reports the common coexistence of andalusite and sillimanite in a septum of Lower Devonian Littleton Formation pelites (the Moosilauke septum) within Kinsman Quartz Monzonite–Bethlehem Gneiss plutonic rocks, and the widespread occurrence of kyanite in rocks of the Silurian Clough Formation less than 5 km to the west in

the vicinity of Black Mountain (Fig. 2). The trace of the Al_2SiO_5 isobar as defined by Thompson and Norton (1968) is within the septum and passes near Hurricane Mountain and Mt. Moosilauke.

The *P–T* conditions of the Moosilauke septum relative to the Al_2SiO_5 triple point can be ascertained from the distribution of Al_2SiO_5 polymorphs shown in Figure 2 and the topology of the Al_2SiO_5 phase diagram provided that: (1) all of the aluminum silicates in this area crystallized during a single metamorphic episode, and (2) the andalusite + sillimanite assemblages were at stable rather than metastable equilibrium. Rumble (1973) reports evidence for multiple episodes of aluminosilicate crystallization in the Moosilauke septum; specifically, he describes the sequence andalusite → prismatic + fibrolitic sillimanite → andalusite. Rumble concludes that this occurred during a single metamorphic episode and that metamorphic conditions were never far removed from the andalusite–sillimanite univariant equilibrium.

Given the distribution of andalusite and silliman-

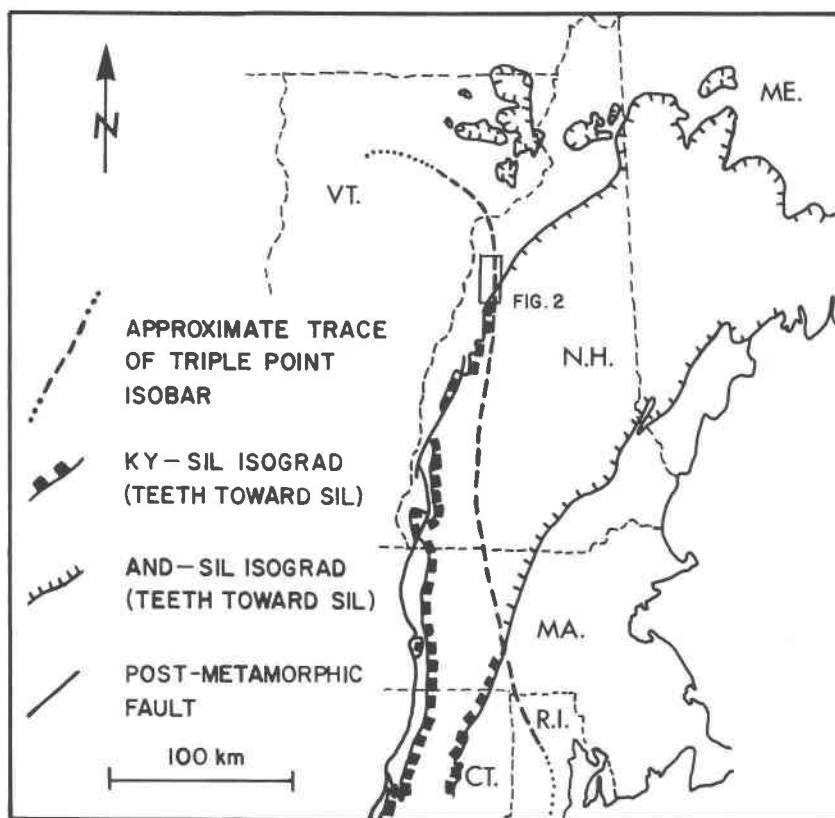

Fig. 1. Map of central New England showing the trace of the Al_2SiO_5 isobar, the kyanite–sillimanite isograd and the andalusite–sillimanite isograd (after Thompson and Norton, 1968). Box shows location of study area (Fig. 2).
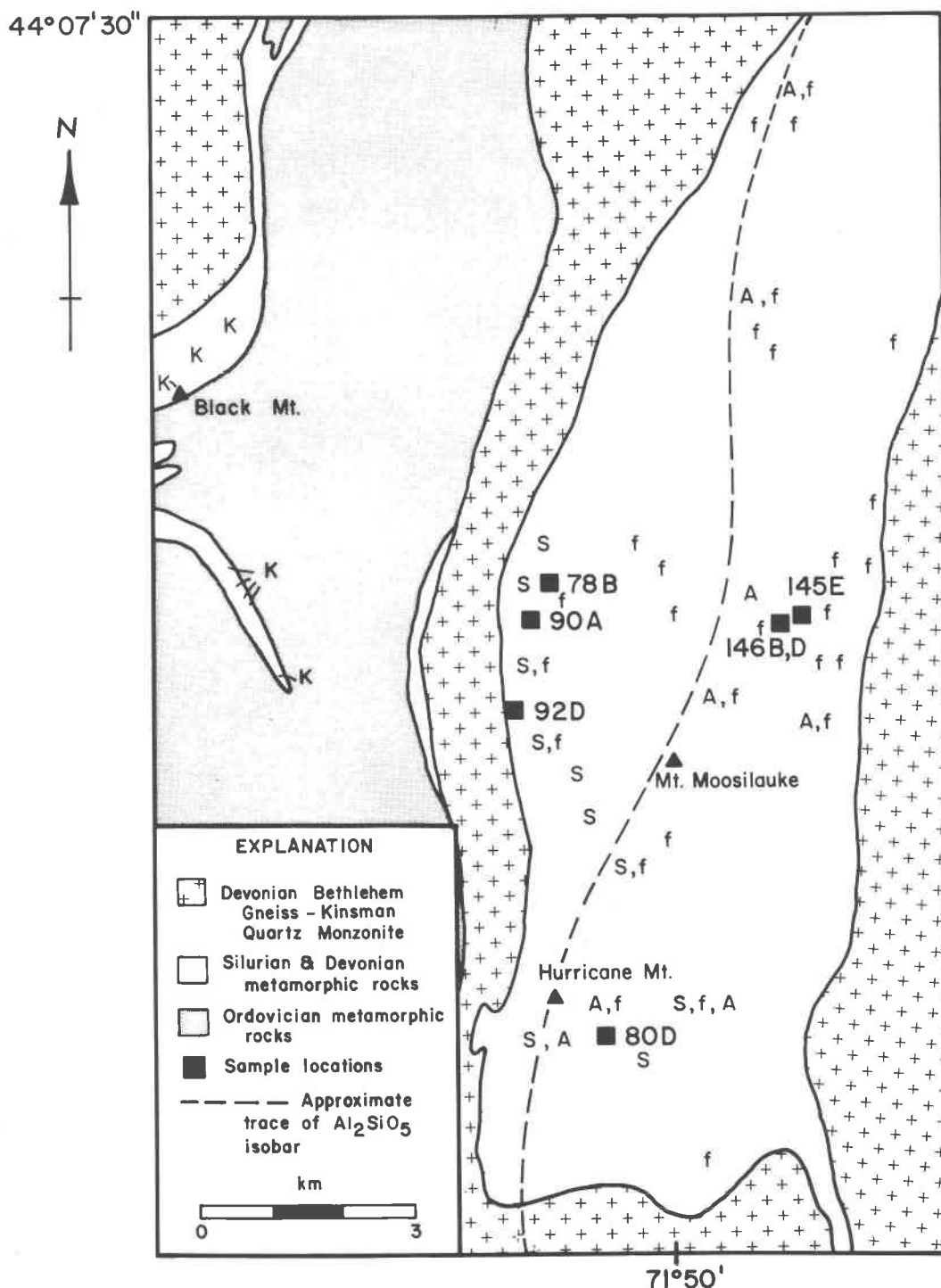
Fig. 2. Geologic map of the study area showing sample localities, distribution of rock units, and Al_2SiO_5 polymorphs. The large belt of Silurian and Devonian metamorphic rocks on the right of the map (no pattern) is the Moosilauke septum and consists predominantly of Devonian Littleton Formation. Abbreviations are K = kyanite, S = prismatic sillimanite, f = fibrolite and A = andalusite. The order of Al_2SiO_5 polymorphs listed on the map at any one locality indicates the sequence of progressive crystallization (e.g., S, f, A means prismatic sillimanite was followed by growth of fibrolite and then andalusite). After Rumble (1973).

ite in the Moosilauke septum shown in Figure 2 and assuming that coexistence of these two phases represents near univariant conditions, the Al_2SiO_5 isobar must pass through the septum as indicated by Thompson and Norton (1968), or just to the west of the septum in the Bethlehem gneiss. The total absence of any reported kyanite in the Moosilauke septum argues for the latter interpretation. In this case the andalusite + sillimanite coexistence within the septum requires temperatures slightly above, and pressures slightly below, those of the triple point. Therefore, we conclude that peak metamorphic temperatures in the Moosilauke septum were at, or slightly above, and pressures were at, or slightly below, those of the Al_2SiO_5 triple point.

Sample selection and analytical techniques

We selected seven samples of pelitic schist from the Moosilauke area, collected and generously contributed by Douglas Rumble III, for detailed geothermometric and geobarometric study. Our choice of samples was based on the presence of aluminum silicate minerals and plagioclase in order to maximize the number of applicable geothermometers and geobarometers. The mineralogy of each sample is given in Table 1, and sample locations are shown in Figure 2.

Major element analyses were obtained for garnet, biotite, muscovite, plagioclase, and staurolite using the automated Materials Analysis Corporation electron microprobe at MIT. The following analytical technique was used to increase the probability that the analyzed compositions are representative of equilibrium compositions at peak metamorphic conditions. Two to three domains were identified in each polished thin section such that, in each domain, all minerals to be analyzed were in contact or, in exceptional cases, less than 1 mm apart. Mineral rims were then analyzed at points of mutual contact. For each mineral grain, two to four such analyses were averaged to arrive at mean compositions in each domain. Reproducibility for a given grain was generally better than 3% for major elements. The mineral compositions reported in Tables 2–4 represent the means of the domain averages for each sample.

Spot checks revealed no significant zonation in any of the analyzed minerals. In particular, compositional variations in garnet are limited to less than 0.05 mole fraction for each element; in most cases, this is within the analytical uncertainty of the microprobe.

Table 1. Pelitic schist assemblages from the Moosilauke septum

	78B	80D	90A	92D	145E	146B	146D
Quartz	x	x	x	x	x	x	x
Muscovite	x	x	x	x	x	x	x
Biotite	x	x	x	x	x	x	x
Chlorite		x	x			x	x
Plagioclase	x	x	x	x	x	x	x
Garnet	x	x	x	x	x	x	x
Sillimanite	x	x	x	x	x	x	x
Andalusite						x	x
Staurolite	x		x	x		x	x
Ilmenite	x	x	x	x	x	x	x
Graphite	x	x	x	x	x	x	x

Petrographic observations and phase equilibria

Petrography

Rumble (1973) provides an excellent general discussion of the textural relationships encountered in rocks from this area; the following observations are of specific importance to this study. In all but one of the samples we studied, garnet occurs in equant, euhedral to subhedral porphyroblasts that show little sign of resorption or retrogradation. In contrast, garnets in one sample (146D) preserve no euhedral faces and generally appear broken or rounded in thin section.

Plagioclase occurs in all samples as subhedral porphyroblasts up to 3 mm across. Sericitization and sausseritization are minimal.

Chlorite occurs as irregular, anhedral to subhedral patches in a few of the samples, and is generally associated with late-stage, cross-cutting shear zones (~1 mm wide), although some may be primary. These shear zones were religiously avoided during the study, and chlorite will not be considered further.

Sillimanite occurs in two forms in these samples. Slightly subhedral prismatic grains up to 4 mm across occur in samples 78B, 80D, and 92D. Fibrolite, generally intergrown with muscovite, occurs in 78B, 90A, 92D, 145E, 146B, and 146D.

Andalusite occurs as subhedral to anhedral porphyroblasts up to 5 mm across in samples 146B and D. In both cases, the grains are highly sieved with numerous inclusions of quartz and biotite.

Staurolite forms tiny euhedra (≤0.5 mm) in samples 78B, 92D and 146B, and slightly larger subhedra (up to 1 mm) in samples 90A and 146D. In

Table 2. Electron microprobe analyses of garnet and staurolite

	GARNET							STAUROLITE			
	78B	80D	90A	92D	145E	146B	146D	78B	90A	92D	146B
SiO$_2$	38.53	36.37	37.27	37.10	36.68	36.62	37.95	27.45	29.17	28.79	28.42
Al$_2$O$_3$	21.85	21.39	21.03	21.39	20.95	21.17	21.36	54.54	55.01	53.84	54.57
TiO$_2$	–	0.01	0.10	0.01	0.10	0.02	0.12	0.62	0.54	0.55	0.57
MgO	2.30	2.20	2.46	2.38	2.00	2.99	2.45	1.52	1.22	1.47	1.37
FeO	33.77	33.51	32.44	34.07	34.30	30.48	30.39	13.55	11.99	12.93	10.84
MnO	4.86	4.02	6.08	4.92	5.47	7.09	7.44	0.25	0.26	0.24	0.37
ZnO	n.d.	n.d.	n.d.	n.d.	n.d.	n.d.	n.d.	0.20	0.16	0.32	2.50
CaO	0.87	1.86	1.03	0.72	0.54	1.33	1.33	0.01	0.01	0.02	0.02
	102.18	99.36	100.41	100.59	100.04	99.70	101.04	98.13	98.36	98.16	98.65
	FORMULA BASIS 12 OXYGENS							FORMULA BASIS 23 OXYGENS			
Si	3.034	2.964	3.003	2.989	2.987	2.968	3.024	3.806	3.986	3.971	3.911
Al	2.028	2.057	1.998	2.032	2.011	2.023	2.006	8.913	8.861	8.753	8.851
Ti	–	–	0.006	0.001	0.006	0.001	0.007	0.081	0.070	0.072	0.073
Mg	0.270	0.267	0.296	0.286	0.242	0.361	0.290	0.313	0.249	0.302	0.282
Fe	2.224	2.282	2.187	2.295	2.336	2.066	2.026	1.572	1.370	1.492	1.247
Mn	0.324	0.277	0.415	0.336	0.377	0.487	0.502	0.029	0.030	0.028	0.044
Zn	n.d.	n.d.	n.d.	n.d.	n.d.	n.d.	n.d.	0.020	0.016	0.032	0.254
Ca	0.074	0.163	0.089	0.062	0.047	0.115	0.113	0.002	0.002	0.003	0.003
	7.954	8.009	7.994	7.996	8.006	8.021	7.968	14.736	14.584	14.653	14.665
$\dfrac{Fe}{Fe+Mg}$	0.892	0.895	0.881	0.889	0.906	0.851	0.875	0.834	0.846	0.832	0.816
X_{Al}	0.769	0.764	0.732	0.772	0.778	0.682	0.691				
X_{PY}	0.093	0.091	0.099	0.096	0.081	0.119	0.099				
X_{GR}	0.026	0.055	0.030	0.021	0.016	0.038	0.039				
X_{SP}	0.112	0.090	0.139	0.111	0.126	0.161	0.171				

sample 92D, staurolite and muscovite rim prismatic sillimanite, suggesting the retrograde reaction:

sillimanite + biotite + H$_2$O

$\rightarrow$ staurolite + muscovite + quartz

(Billings, 1937; Rumble, 1973).

Phase equilibria

Figure 3 is an AFM projection (after Thompson, 1957) of mineral assemblages from the Moosilauke septum. In general, there is a systematic distribution of Al, Fe, and Mg among coexisting phases, with the exception of sample 80D. Most notable on the figure, however, is the systematic displacement of the seven garnet + biotite + Al$_2$SiO$_5$ assemblages with respect to Fe/Mg. Figure 4, which is a projection from quartz, muscovite, Al$_2$SiO$_5$ and H$_2$O into the tetrahedron Fe–Mg–Ca–Na, shows that there is a systematic increase in the Ca contents of garnet and coexisting plagioclase with decreasing Fe/Mg. The one exception is sample 80D,

which has the highest Ca content, and relatively high Fe/Mg. A similar projection into the tetrahedron Fe–Mg–Ca–Mn (not shown) reveals that the most manganiferous garnets are those with the lowest Fe/Mg, again with the exception of sample 80D. Thus, the systematic displacement of the three phase assemblages garnet–biotite–Al$_2$SiO$_5$ on the AFM projection (Fig. 3) can be explained by consideration of the additional components Ca and Mn. The fact that sample 80D reveals crossing tie-line relations indicates that this sample could not have crystallized in equilibrium with the other assemblages, although there is no obvious textural evidence for disequilibrium. Despite compositional evidence for disequilibrium, geothermometry and geobarometry on 80D (see below) yields temperatures and pressures consistent with the other samples because of compensating factors in the calculation of the equilibrium constants. This reveals an important point: consistency of calculated temperatures and pressures cannot necessarily be taken as evidence for equilibrium.

Table 3. Electron microprobe analyses of biotite and muscovite

	BIOTITE							MUSCOVITE						
	78B	80D	90A	92D	145E	146B	146D	78B	80D	90A	92D	145E	146B	146D
SiO_2	36.31	35.18	35.65	35.45	34.79	36.28	36.17	47.49	46.77	46.63	46.99	46.76	46.39	46.88
Al_2O_3	19.74	19.52	19.76	19.91	19.61	19.90	19.93	35.84	36.51	36.14	36.95	36.38	35.79	36.08
TiO_2	1.43	1.25	1.29	1.38	1.40	1.40	1.30	0.43	0.51	0.42	0.66	0.34	0.40	0.52
MgO	10.04	9.77	10.40	9.85	8.57	11.14	11.17	0.48	0.49	0.48	0.49	0.45	0.40	0.53
FeO	18.35	20.15	18.24	19.19	20.53	17.19	17.21	0.74	0.94	0.73	0.80	0.83	0.80	0.74
MnO	0.12	0.11	0.13	0.10	0.17	0.09	0.18	-	0.02	0.02	-	0.05	0.01	0.01
CaO	0.11	0.01	0.01	0.05	0.06	0.07	0.06	0.07	0.02	0.03	0.02	0.03	0.03	0.03
Na_2O	0.28	0.19	0.28	0.45	0.42	0.45	0.33	1.78	1.26	1.73	1.91	1.68	1.34	1.38
K_2O	7.90	8.27	8.12	7.87	8.15	8.00	8.23	8.29	9.22	8.43	8.57	8.58	8.70	8.94
	94.28	94.45	93.88	94.25	93.70	94.52	94.58	95.12	95.74	94.61	96.39	95.10	93.86	95.11

CATIONS PER 22 OXYGENS

Si	5.489	5.385	5.428	5.397	5.385	5.448	5.437	6.241	6.142	6.171	6.115	6.165	6.192	6.183
Al^{IV}	2.511	2.615	2.572	2.603	2.615	2.552	2.563	1.759	1.858	1.829	1.885	1.835	1.808	1.817
Al^{VI}	1.008	0.907	0.975	0.970	0.964	0.971	0.969	3.793	3.795	3.811	3.784	3.819	3.824	3.792
Ti	0.163	0.145	0.147	0.158	0.158	0.158	0.147	0.043	0.050	0.042	0.065	0.033	0.040	0.052
Mg	2.262	2.228	2.360	2.235	1.977	2.494	2.502	0.093	0.095	0.095	0.095	0.089	0.080	0.104
Fe	2.320	2.580	2.322	2.443	2.659	2.159	2.163	0.081	0.103	0.081	0.087	0.091	0.089	0.082
Mn	0.015	0.014	0.016	0.013	0.023	0.012	0.023	-	0.002	0.002	-	0.005	0.001	0.001
ΣVI	5.768	5.874	5.820	5.819	5.784	5.794	5.804	4.010	4.045	4.031	4.031	4.037	4.034	4.031
Ca	0.018	0.001	0.002	0.008	0.009	0.012	0.010	0.010	0.003	0.004	0.003	0.004	0.004	0.004
Na	0.082	0.057	0.083	0.133	0.125	0.130	0.096	0.453	0.321	0.442	0.482	0.434	0.347	0.353
K	1.524	1.616	1.577	1.528	1.610	1.533	1.577	1.389	1.544	1.424	1.423	1.442	1.480	1.505
ΣA	1.624	1.674	1.662	1.670	1.744	1.675	1.683	1.852	1.868	1.870	1.908	1.880	1.833	1.862
$\frac{Fe}{Fe+Mg}$	0.506	0.537	0.496	0.522	0.574	0.464	0.464	0.466	0.520	0.460	0.478	0.506	0.529	0.441

Staurolite is also present in four of the samples, as shown in Figure 3. The presence of staurolite as an "extra phase" on the AFM projection cannot be explained by consideration of additional components (for example, there is very little Zn present in these staurolites). However, the presence of staurolite is consistent with the notion that the chemical potential of H_2O is internally buffered by the mineral assemblages. As will be shown later, calculations of fluid-dependent equilibria involving staurolite are also consistent with $P(H_2O) < P_{total}$ in these assemblages. It should also be pointed out that presence of Mn and Ca in the garnet allows reaction between staurolite, muscovite, sillimanite, biotite, and garnet to take place over a limited range of temperatures.

Methods of pressure and temperature estimation

"Peak" metamorphic temperatures and pressures at Mt. Moosilauke can be estimated in two fundamental ways: (1) through comparison with experimental determinations of the aluminosilicate invariant point, and (2) through the application of continuous equilibria that have been calibrated as geothermometers and geobarometers.

Table 4. Electron microprobe analyses of plagioclase

	78B	80D	90A	92D	145E	146B	146D
SiO_2	65.19	61.32	64.93	65.25	66.24	62.03	61.75
Al_2O_3	21.21	24.89	22.58	21.73	21.66	23.60	24.14
FeO	0.03	0.15	0.55	0.23	0.40	0.41	0.41
CaO	2.65	5.73	2.91	2.24	1.90	5.02	5.10
Na_2O	10.95	8.09	9.37	10.50	10.68	8.64	8.68
K_2O	0.11	0.09	0.44	0.06	0.07	0.08	0.09
	100.14	100.27	100.78	100.01	100.95	99.78	100.17

FORMULA BASIS 8 OXYGENS

Si	2.871	2.714	2.843	2.878	2.887	2.758	2.738
Al	1.102	1.299	1.166	1.126	1.113	1.237	1.262
Fe	0.010	0.006	0.020	0.010	0.015	0.015	0.016
Ca	0.125	0.272	0.136	0.106	0.090	0.239	0.243
Na	0.935	0.694	0.795	0.873	0.903	0.745	0.746
K	0.006	0.006	0.025	0.003	0.004	0.005	0.005
Total	5.049	4.991	4.985	4.996	5.012	4.999	5.010
X_{AN}	0.116	0.278	0.139	0.107	0.089	0.238	0.241
X_{AB}	0.869	0.710	0.815	0.880	0.892	0.742	0.739
X_{OR}	0.006	0.006	0.026	0.003	0.004	0.005	0.005

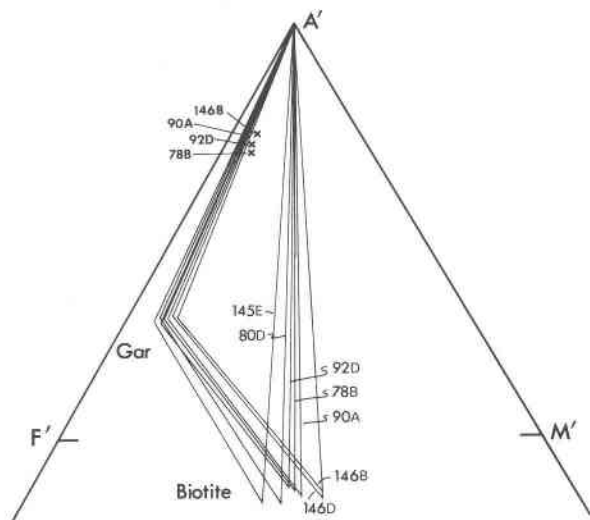Fig. 3. AFM projection from quartz, muscovite, and H_2O of assemblages from the Moosilauke septum. Sample numbers are indicated for each assemblage and staurolite is indicated by the symbol X. Tie lines to staurolite have not been drawn for the sake of clarity.

P–T coordinates of the Al_2SiO_5 triple point

The aluminosilicate invariant point is one of the few in natural systems that involves only essentially pure phases. As such, it offers the rare opportunity to uniquely constrain pressure and temperature conditions through petrographic observation alone. Unfortunately, the position of the Al_2SiO_5 invariant

point in P–T space has been the subject of considerable debate (see Zen, 1969, and Anderson et al., 1977, for succinct reviews), and there is still controversy over which value to accept. Anderson et al. (1977) point out that Holdaway's experiments are the only ones consistent with all of the available thermodynamic data, and Helgeson et al. (1978) arrive at a similar conclusion. Consequently, we will adopt Holdaway's estimates of 501±20°C and 3760±300 bars for the P–T coordinates of the aluminosilicate triple point.

In assigning these conditions to the Mt. Moosilauke area we ignore the possible complicating effects of additional components in the aluminosilicate minerals. Strens (1968) and Althaus (1969), among others, have expressed concern that ferric iron content could have a significant effect on Al_2SiO_5 equilibrium. Rumble (1973) presents Fe_2O_3 analyses for eleven aluminosilicates from the Moosilauke area, which range from 0.12 to 0.42 wt.%. These values fall well within the range of ferric iron contents reported by Holdaway (1971).

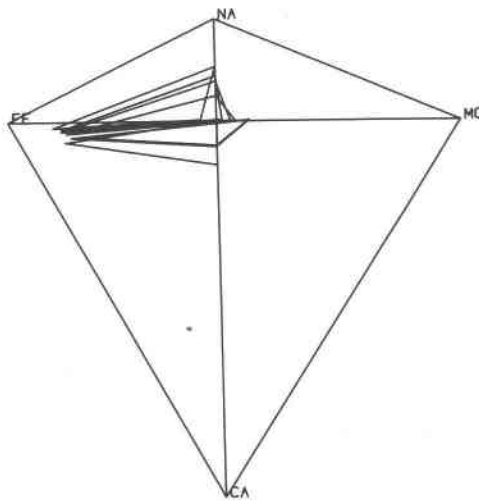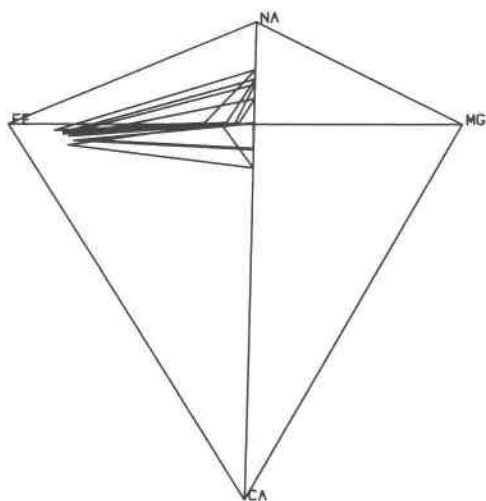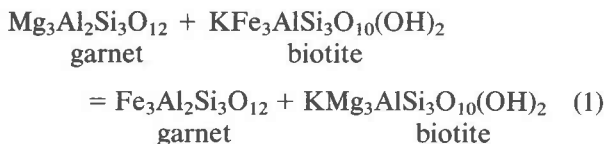## Garnet–biotite geothermometry

The cation exchange reaction:

$$Mg_3Al_2Si_3O_{12} + KFe_3AlSi_3O_{10}(OH)_2$$
$$\quad \text{garnet} \qquad\qquad \text{biotite}$$

$$= Fe_3Al_2Si_3O_{12} + KMg_3AlSi_3O_{10}(OH)_2 \quad (1)$$
$$\qquad \text{garnet} \qquad\qquad \text{biotite}$$

Fig. 4. Stereoscopic projection (Spear, 1980) from quartz, muscovite, Al_2SiO_5 and H_2O into the tetrahedron Fe–Mg–Ca–Na showing the distribution of tie lines among garnet (which plots closest to the Fe apex), biotite (which plots along the Fe–Mg join) and plagioclase (which plots along the Ca–Na join). Assemblages in order in increasing Ca content in plagioclase are: 145E, 92D, 78B, 90A, 146B, 146D, 80D.

has been calibrated as a geothermometer by Thompson (1976), Goldman and Albee (1977), and Ferry and Spear (1978). Thompson's empirical calibration is based largely on comparison of natural assemblages with experimental phase equilibria. Goldman and Albee based their calibration on temperatures derived from quartz–magnetite oxygen isotope exchange geothermometry. The Ferry and Spear calibration is based on experiments in the purely binary Fe–Mg system. Field application of the Ferry–Spear calibration can be hampered by significant deviations from the idealized system (Ferry and Spear, 1978). The Thompson and Goldman–Albee calibrations probably minimize compositional effects since they are based on natural assemblages, but neither corrects for the effects of pressure on the equilibrium. Furthermore, both of these calibrations may be affected by the propensity of garnet and biotite to reequilibrate during cooling at geologically reasonable rates, and may thus significantly underestimate metamorphic temperatures. This problem is strongly amplified in the Goldman–Albee calibration inasmuch as both Fe–Mg and ^{18}O–^{16}O exchange may have occurred at different rates during cooling. Reequilibration during cooling should be more pronounced in higher grade assemblages, and indeed, all three garnet–biotite calibrations agree reasonably well at low temperatures. At conditions comparable to those of the Al_2SiO_5 triple point, the Thompson and Ferry–Spear calibrations yield virtually indistinguishable results.

Because it expressly accounts for pressure effects, we will use the Ferry–Spear calibration:

$$0 = 12454 - 4.662T(°K) + 0.057P(bars)$$
$$+ RT(°K)\ln K_1$$

where[2]

$$K_1 = \frac{(X_{py})^3(X_{ann})^3}{(X_{ph})^3(X_{al})^3}$$

assuming ideal solution.

Garnet–plagioclase–Al_2SiO_5–quartz geobarometry

The equilibrium relation:

$$Ca_3Al_2Si_3O_{12} + 2Al_2SiO_5 + SiO_2$$
garnet   Al–Si   quartz

$$= 3CaAl_2Si_2O_8   (2)$$
plagioclase

---
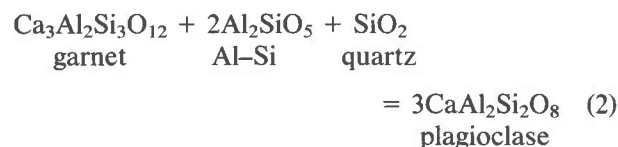
has been calibrated as a geobarometer by Ghent (1976) using available thermochemical data. For sillimanite-bearing assemblages, the expression is:

$$0 = 11675 - 32.815T(°K) + 1.301[P(bars) - 1]$$
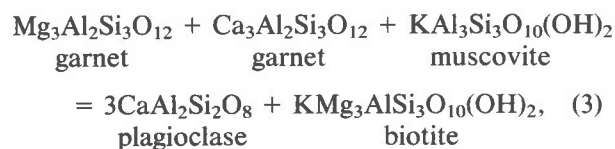$$+ RT(°K)\ln K_2.$$

Whereas Ferry and Spear (1978) treated garnet solid solution as ideal in their calibration of Equilibrium 1, Ghent (1976) and subsequent authors have emphasized the need to account for the non-ideality of garnet as well as plagioclase solid solutions when applying Equilibrium 2. The equilibrium constant for this equation can be expressed as:

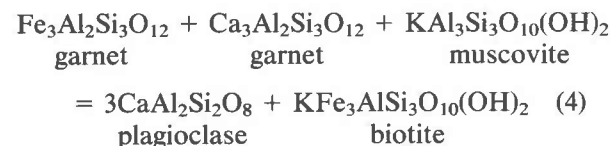$$K_2 = \frac{(X_{an})^3(\gamma_{an})^3}{(X_{gr})^3(\gamma_{gr})^3} = (K_{2i})(K_{2ni})$$

where K_{2i} and K_{2ni} are the "ideal" and "non-ideal" components of K_2, respectively. Pointing out that the necessary activity coefficients are rather poorly known, Ghent *et al.* (1979) suggested an empirical method for estimating the effects of non-ideal solution behavior on Equilbrium 2. It was assumed that lines of constant K_D for the equilibrium grossular + kyanite + quartz = anorthite were approximately parallel to Holdaway's (1971) kyanite–sillimanite curve. K_{2i} was calculated for a number of samples that straddled a kyanite–sillimanite isograd. K_{2ni} was then calculated such that the P–T curve for Equilibrium 2 would coincide with the kyanite–sillimanite boundary. This approach yields $K_{2ni} = 2.5$, a value which we will adopt here.

Garnet–muscovite–plagioclase–biotite geobarometry

The equilibrium relation:

$$Mg_3Al_2Si_3O_{12} + Ca_3Al_2Si_3O_{12} + KAl_3Si_3O_{10}(OH)_2$$
garnet   garnet   muscovite

$$= 3CaAl_2Si_2O_8 + KMg_3AlSi_3O_{10}(OH)_2,   (3)$$
plagioclase   biotite

and its Fe counterpart:

$$Fe_3Al_2Si_3O_{12} + Ca_3Al_2Si_3O_{12} + KAl_3Si_3O_{10}(OH)_2$$
garnet   garnet   muscovite

$$= 3CaAl_2Si_2O_8 + KFe_3AlSi_3O_{10}(OH)_2   (4)$$
plagioclase   biotite

involve Ca partitioning between coexisting garnet and plagioclase similar to Equilibrium 2 and should also be pressure sensitive. Ghent and Stout (1981) have presented an empirical calibration of these two

equilibria using natural samples from the Water-ville–Vassalboro area, Maine (Ferry, 1980) and the Mica Creek area, British Columbia, for which P and T have been estimated using Equilibria 1 and 2. Their results are:

$$0 = -8888.4 - 16.675T(°K) + 1.738P(bars)$$
$$+ RT(°K)\ln K_3$$

and

$$0 = 4124.4 - 22.061T(°K) + 1.802P(bars)$$
$$+ RT(°K)\ln K_4$$

where

$$K_3 = \frac{(X_{an})^3(X_{ph})^3}{(X_{mu})(X_{py})^3(X_{gr})^3}$$

and

$$K_4 = \frac{(X_{an})^3(X_{ann})^3}{(X_{mu})(X_{al})^3(X_{gr})^3}.$$

These formulations for K_3 and K_4 utilize ideal ionic solution models for the various phases with the effects of non-ideality being accounted for by the numerical coefficients in the equilibrium constant equations. It should be noted that these values, which are based on P–T estimates from garnet–biotite and garnet–plagioclase–Al_2SiO_5–quartz equilibria, rely completely on the accuracy of these calibations; consequently, they carry large uncertainties.

Plagioclase–muscovite–Al_2SiO_5–quartz–H_2O geothermometry

The equilibrium:

$$NaAl_3Si_3O_{10}(OH)_2 + SiO_2 = NaAlSi_3O_8$$
$$\text{muscovite} \qquad \text{quartz} \qquad \text{albite}$$
$$+ Al_2SiO_5 + H_2O \quad (5)$$
$$\text{Al–Si}$$
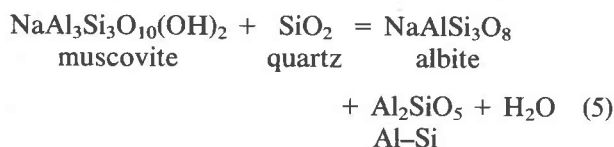
has been calibrated as a geothermometer by Cheney and Guidotti (1979) based on the experimental results of Chatterjee (1972). The equilibrium expression is:

$$0 = 22057.11 - 40.67T(°K) + 0.1069[P(bars) - 1]$$
$$+ RT(°K)\ln K_5$$

and

$$K_5 = \frac{(X_{ab})(\gamma_{ab})}{(X_{pa})(\gamma_{pa})} \cdot f(H_2O)$$

If one assumes $\gamma_{ab} = 1.0$ (Orville, 1972) and an asymmetric solution model for muscovite solid solution,

$$-\ln K_5 = \ln(X_{pa}) - \ln(X_{ab}) - \ln[f(H_2O)]$$
$$+ (X_{mu})^2/RT[W_{pa}+2(X_{pa})(W_{mu}-W_{pa})].$$

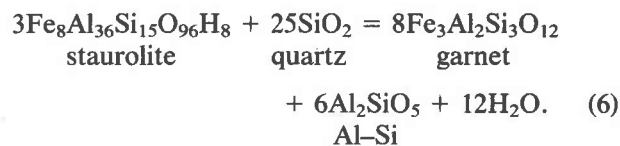Chatterjee and Froese (1975) estimate the necessary Margules parameters as:

$$W_{pa} = 2923.1 + 0.1590P(bars) + 0.1698T(°K),$$

and
$$W_{mu} = 4650.1 - 0.1090P(bars) + 0.3954T(°K).$$

Garnet–staurolite–Al_2SiO_5–quartz–H_2O geothermometry

Iron partitioning between garnet and staurolite in the presence of sillimanite and quartz can be described by:

$$3Fe_8Al_{36}Si_{15}O_{96}H_8 + 25SiO_2 = 8Fe_3Al_2Si_3O_{12}$$
$$\text{staurolite} \qquad \text{quartz} \qquad \text{garnet}$$
$$+ 6Al_2SiO_5 + 12H_2O. \quad (6)$$
$$\text{Al–Si}$$

Based on the experimental data of Richardson (1968), Hutcheon (1979) suggests the calibration:

$$0 = 1571113 - 1837.668T(°K) - 0.897[P(bars)-1]$$
$$+ RT(°K)\ln K_6$$

Using the ideal activity–composition formulation of Hutcheon (1979), K_6 is calculated as:

$$K_6 = \frac{(X_{al})^{24}}{(X_{Fe})^{24}} \cdot f(H_2O)^{12}$$

Results

Using data from Tables 2–4 and the formulae given in Table 5 for calculating the mole fractions of phase components, equilibrium constants were generated for the continuous reactions described in the previous section. If a standard error (σ) of 3% is assumed for the microprobe data, then the standard error for an equilibrium constant of the form $K = f(A,B,C,D . . .)$ is:

$$\sigma_K^2 = (\partial K/\partial A)^2 (\sigma_A)^2 + (\partial K/\partial B)^2 (\sigma_B)^2 + (\partial K/\partial C)^2 (\sigma_C)^2 + (\partial K/\partial D)^2 (\sigma_D)^2 . . .$$

(Smith, 1966, p. 174). For the Moosilauke septum data, this formulation yields $\sigma_{K1} \simeq 0.16$, $\sigma_{K2} \simeq 0.16$, $\sigma_{K3} \simeq 0.21$, and $\sigma_{K4} \simeq 0.18$, or approximately ±4–5% of the value of K. Rigorous error analysis was

Table 5. Formulae used to calculate mole fractions of phase components

$X_{al} = Fe/(Fe + Mg + Ca + Mn)$ $X_{an} = Ca/(Ca + Na + K)$

$X_{py} = Mg/(Fe + Mg + Ca + Mn)$ $X_{ab} = Na/(Ca + Na + K)$

$X_{gr} = Ca/(Fe + Mg + Ca + Mn)$ $X_{mu} = (X_K)(X_{AlVI})^2$

$X_{Fe} = Fe/(Fe + Mg + Mn + Zn)$ $X_{pa} = (X_{Na})(X_{AlVI})^2$

$X_{ann} = Fe/(Fe + Mg + Ti + Al^{VI})$ $X_K = K/(Ca + Na + K)$

$X_{ph} = Mg/(Fe + Mg + Ti + Al^{VI})$ $X_{Na} = Na/(Ca + Na + K)$

$$X_{AlVI} = Al^{VI}/(Fe + Mg + Mn + Ti + Al^{VI})$$

al = almandine, py = pyrope, gr = grossular, Fe = Fe end-member staurolite, ann = annite, ph = phlogopite, an = anorthite, ab = albite, mu = muscovite, pa = paragonite.

not attempted for fluid-dependent equilibria because uncertainties in $f(H_2O)$ far outweigh analytical uncertainties for these reactions.

Pressure–temperature curves for fluid-independent reactions, calculated using the equilibrium constants for each sample, are shown in Figure 5 and diagrams depicting the intersection of Equilibrium 1 (garnet–biotite) with Equilibria 2, 3 and 4 are presented in Figure 6. The two lines shown in

Figure 5 for each equilibrium represent one standard deviation in the equilibrium constant as calculated above, and do not reflect possible errors in calibration. The overall uncertainties of the calculated pressures and temperatures will be larger than these error brackets.

From Figures 5 and 6 it can be seen that temperatures calculated from the garnet–biotite geothermometer as calibrated by Ferry and Spear (1978) are entirely consistent with Holdaway's estimated triple point temperature. Temperatures calculated using this equilibrium are within analytical error of 501°C for all but two samples (78B and 146D), and in these cases the analytical error brackets overlap Holdaway's reported error for the triple point temperature (±20°).

Pressures estimated from simultaneous solutions of Equilibria 1 and 2 (Fig. 6a) are generally in very good agreement with Holdaway's estimate of 3760±300 bars. The one notable exception is sample 146D for which a pressure of 2320±500 bars is calculated using Equilibria 1 and 2. It is perhaps not coincidental that this is the sample that shows the strongest signs of textural disequilibrium.

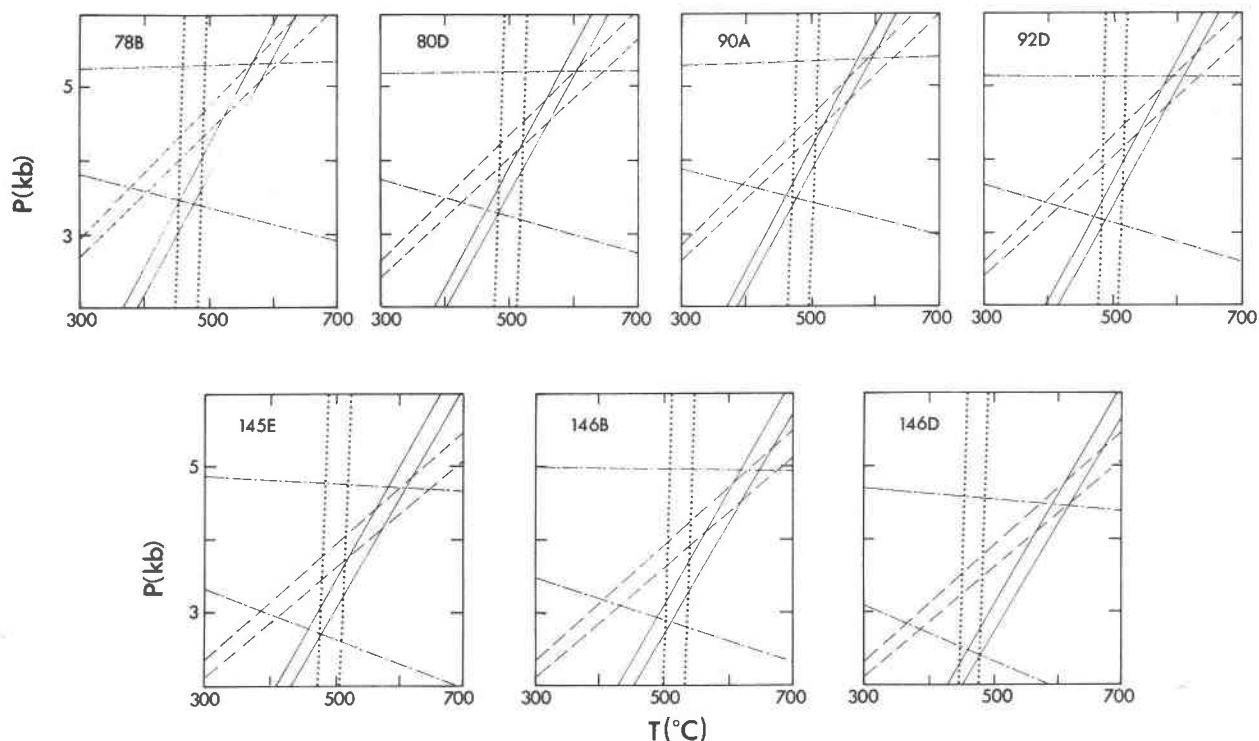The error polygon produced by the intersection

Fig. 5. *P–T* plots of fluid-independent equilibria 1–4 for the studied samples. Dotted curves = equilibrium 1, solid curves = equilibrium 2, dashed curves = equilibrium 3, and dash-dot curves = equilibrium 4. The two curves shown for each equilibrium represent ±1σ based on propagation of 3% standard error in microprobe analyses.
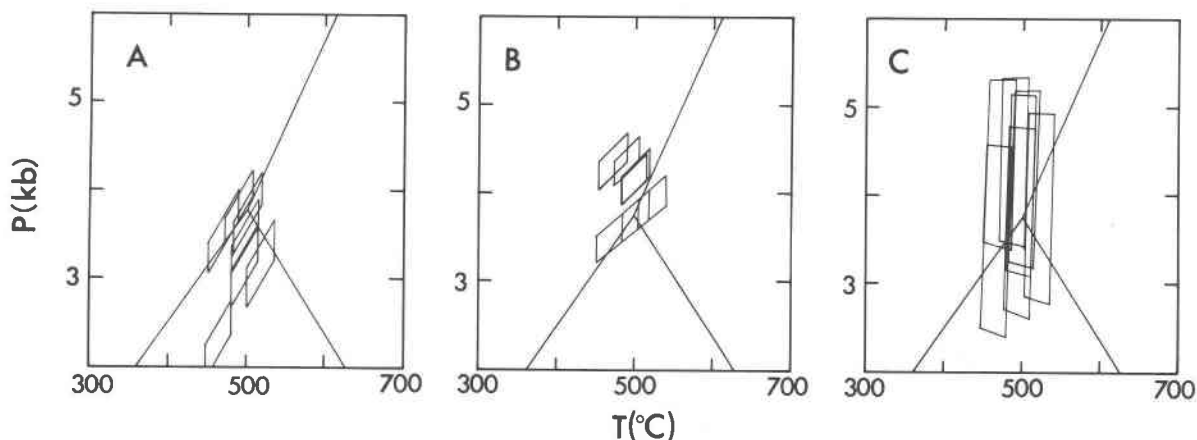
Fig. 6. Synoptic *P–T* diagrams showing simultaneous solutions of equilibria 1 + 2 (a), equilibria 1 + 4 (b), and equilibria 1 + 3 (c) for all samples.

of Equilibria 1 and 4 (Fig. 6b) includes the triple point for sample 145E, and overlaps the triple point error brackets for all other samples except 78B and 90A. Note that, in every case, the Equilibria 1–4 solution estimates higher pressures than the 1–2 solution. This was an unexpected result, considering that Equilibrium 4 was calibrated using Equilibria 1 and 2, and perhaps suggests a slight, but consistent, error in the calibration.

Simultaneous solution of Equilibria 1 and 3 (Fig. 6c) results in pressure estimates for all samples that are consistent with Holdaway's (1971) triple point error brackets. However, propagation of 3% analytical errors yields very large standard errors for calculated pressures ($\pm \sim 1000$ bars), and severely limits the usefulness of this equilibrium for geobarometry in natural systems.

The two fluid dependent equilibria, Equilibria 5 and 6, can be used to estimate metamorphic temperatures if an assumption is made about $P(H_2O)$. All of the samples contain graphite; thus, the maximum $P(H_2O)$ in a C–O–H fluid at triple point pressure–temperature conditions is approximately $0.92P_{total}$ or 3460 bars (Ohmoto and Kerrick, 1977). Assuming this value, temperatures calculated using Equilibria 5 and 6 are 75–150°C higher than those calculated from fluid independent equilibria (Table 6).

A number of workers (*e.g.*, Ghent *et al.*, 1979; Hutcheon, 1979; and Ferry, 1980) have discussed poor calibration as a source of error involving staurolite equilibria, and this must account for at least part of the discrepancy in temperature estimates. Another possibility is crystallization under conditions of $P(H_2O) < P_{total}$. Using the tempera-

tures and pressures calculated from the fluid independent equilibria for each sample, the H_2O fugacities shown in Table 6 are calculated. These values range from approximately 200–600 bars for equilibrium 5 and 10^{-2} to 10^{-5} for equilibrium 6. The fugacity values calculated from Equilibrium 6 are considered to be too low to be geologically reasonable, but the values of 200–600 bars obtained from Equilibrium 5 appear to be quite reasonable and correspond to $P(H_2O) = 0.1$–0.3 of P_{total}. Assuming that $P_{fluid} = P_{total}$, it is possible to calculate the composition of a C–O–H fluid in equilibrium with graphite at this specified value of $f(H_2O)$ (*e.g.*, Ohmoto and Kerrick, 1977). Such a fluid will either be moderately oxidizing ($f_{O2} > QFM$), CO_2-rich and CH_4-poor or moderately reducing ($f_{O2} < QFM$), CO_2-poor and CH_4-rich. Both are geologically reasonable fluid compositions; thus, the calculated low values of $P(H_2O)$ are not inconsistent with $P_{fluid} = P_{total}$. The remarkable feature of these calculations is the similarity of H_2O fugacities over the entire study area. How water fugacity could be maintained at such consistently low values over such an extensive, predominantly pelitic terrain is not at all clear.

Other estimates of P–T conditions in the Moosilauke septum

In a recent study of fluid flow during metamorphism at the Beaver Brook fossil locality on the eastern margin of the Moosilauke septum, Rumble *et al.* (1982) estimate metamorphic temperatures of 600±40°C using a variety of fluid-dependent calc-silicate equilibria and assuming $P_{fluid} = P_{tot} = 3500\pm300$ bars. This estimate is reasonably consist-

ent with the temperatures calculated in the present study using fluid-dependent equilibria, but is about 100° higher than our fluid-independent estimates. Temperatures calculated by Rumble *et al.* (1982) for coexisting alkali feldspars from a pre- to syn-metamorphic quartz monzonite dike in the Littleton Formation are 509 to 529°C, depending on the calibration used for K–Na exchange between plagioclase and microcline. These estimates are comparable to our garnet–biotite values for samples 145E and 146B, which are from the Beaver Brook area. Considering the distribution of aluminosilicates in the Moosilauke septum and the good agreement between garnet–biotite and plagioclase–microcline temperatures, we suggest that the fluid-dependent calc-silicate equilibria may overestimate metamorphic temperatures at Beaver Brook.

Toward a more consistent set of calibrations

Thus far we have used calibrations of geothermometers and geobarometers exactly as they appeared in the literature in order to test their internal consistency. Unfortunately, different calibrations assume different solution behavior for the same mineral systems. For example, the two calibrations that yielded *P–T* estimates that were most consistent with Holdaway's triple point were the Ferry and Spear (1978) calibration of Equilibrium 1 and the Ghent *et al.* (1979) calibration of Equilibrium 2. The former treats garnet solid solution as ideal whereas the latter assumes non-ideality. In this section we present calibrations of these equilibria that adopt a consistent set of solution models. Specifically, we assume non-ideal solution behavior for garnet and plagioclase, ideal Fe–Mg mixing for biotite, and purity for all other phases. Unfortunately, the use of non-ideal models requires the introduction of activity coefficients, which are not always well known for the temperatures and pressures of interest. We can, however, place important constraints on these values through the use of the Mt. Moosilauke data.

Garnet–biotite geothermometry

Mueller (1972) suggested that Fe–Mg solid solution in biotite is nearly ideal. Although this conclusion has been questioned by other workers (*e.g.*, Dallmeyer, 1975), we will assume ideality and suggest caution in applying this geothermometer to samples in which Ti is a major biotite component. Accounting for non-ideality in garnet solid solu-

tions, the equilibrium constant for the garnet–biotite geothermometer becomes:

$$K_1^* = \frac{(a_{py})^3 (a_{ann})^3}{(a_{ph})^3 (a_{al})^3} = \frac{(X_{py})^3 (X_{ann})^3}{(X_{ph})^3 (X_{al})^3} \cdot \frac{(\gamma_{py})^3}{(\gamma_{al})^3}$$

(K_1^* refers to Equilibrium 1, the * differentiates it as the equilibrium constant formulation involving non-ideal activity-composition relations.) Ganguly and Kennedy (1974) suggest a symmetric, four-component solution model for garnet such that:

$$
\begin{aligned}
RT(°K)\ln\gamma_{py} = {} & W_{FeMg}(X_{al})^2 + W_{CaMg}(X_{gr})^2 + \\
& W_{MgMn}(X_{sp})^2 + (W_{FeMg} - W_{CaFe} + \\
& W_{CaMg})X_{al}X_{gr} + (W_{CaMg} - W_{CaMn} + \\
& W_{MgMn})X_{gr}X_{sp} + (W_{FeMg} - W_{FeMn} \\
& + W_{MgMn})X_{al}X_{sp} \quad (7)
\end{aligned}
$$

$$
\begin{aligned}
RT(°K)\ln\gamma_{al} = {} & W_{FeMg}(X_{py})^2 + W_{CaFe}(X_{gr})^2 + \\
& W_{FeMn}(X_{sp})^2 + (W_{FeMg} - W_{CaMg} + \\
& W_{CaFe})X_{py}X_{gr} + (W_{CaFe} - W_{CaMn} + \\
& W_{FeMn})X_{gr}X_{sp} + (W_{FeMg} - W_{MgMn} + \\
& W_{FeMn})X_{py}X_{sp} \quad (8)
\end{aligned}
$$

where W_{ij} are the free energy interaction or Margules parameters for the bounding binary solutions in the quaternary system. Table 7 presents our preferred values for these parameters. Some of these choices are rather universally agreed upon whereas others are the subject of debate. We have attempted to select values that are the most consistent with current experimental data except where the laboratory results are in strong disagreement with geologic data. The most poorly known of these parameters are those pertaining to manganese. We have followed Ganguly and Kennedy (1974) in assuming essentially ideal behavior for the almandine-spessartine and grossular–spessartine binaries, but py-

Table 6. Calculated values for fluid-dependent equilibria

	EQ [5]		EQ [6]	
#	T(°C)*	f(H$_2$O)**	T(°C)*	f(H$_2$O)**
78B	595	194	665	3x10^{-5}
80D	596	400		
90A	591	293	664	3x10^{-4}
92D	597	255	666	2x10^{-4}
145E	598	328		
146B	590	595	667	2x10^{-2}
146D	594	209		

* Temperatures calculated assuming P(H$_2$O) = 0.92P$_{tot}$ = 3460b.

** f(H$_2$O) values calculated using T and P estimates from fluid-independent equilibria.

Table 7. Margules parameters for garnet solid solutions

MARGULES PARAMETER	SOURCE
$W_{FeMg} = 0$	Newton and Haselton (1981)
$W_{CaMg} = 3300 - 1.5T(^{\circ}K)$	Newton, et al. (1977)
$W_{MgMn} = 0$	This Study
$W_{CaFe} = 0$	Cressey, et al. (1978)
$W_{CaMn} = 0$	Ganguly and Kennedy (1974)
$W_{FeMn} = 0$	Ganguly and Kennedy (1974)

rope–spessartine solutions seem more problematic. We can use the Mt. Moosilauke data to constrain the value of W_{MgMn} at P–T conditions near those of the aluminum silicate triple point. Substituting Margules parameters from Table 7 into equations (7) and (8), we find that:

$$\frac{(\gamma_{py})}{(\gamma_{al})} = \exp$$

$$\left(\frac{[3300 - 1.5(T^{\circ}K)](X_{gr}^2 + X_{al}X_{gr} + X_{gr}X_{sp} + X_{py}X_{gr})}{RT(^{\circ}K)} \right.$$

$$\left. + \frac{W_{MgMn}(X_{sp}^2 + X_{gr}X_{sp} + X_{al}X_{sp} + X_{py}X_{sp})}{RT(^{\circ}K)} \right) \quad (9)$$

Table 8 shows temperatures obtained for the Mt. Moosilauke samples assuming $P = 3760$ bar and using the Ferry and Spear calibration with K_1^* calculated for various values of W_{MgMn}. Ganguly and Kennedy's (1974) suggestion of 3500 cal/mol for this parameter leads to significant overestimates of metamorphic conditions in the Moosilauke septum as inferred from Holdaway's triple point. In fact, only the assumption of $W_{MgMn} \sim 0$ yields reasonable temperatures, suggesting that pyrope–spessartine solutions are effectively ideal at these P–T conditions. In addition, $W_{MgMn} \sim 0$ gives the smallest range of temperatures for rocks which presumably formed at about the same temperature.

Garnet–plagioclase–Al₂SiO₅–quartz geobarometry

Newton and Haselton (1981) have recently presented a new calibration for Equilibrium 2 based on Goldsmith's (1980) experimental determination of the end-member reaction. Since it is based on more recent experimental data than that of Ghent (1976) and Ghent et al. (1979), this calibration will be used

in the discussion to follow. The equilibrium coefficient equation becomes:

$$0 = 9192 - 30.786T(^{\circ}K) + \Delta\overline{V}P(bars)$$
$$+ RT(^{\circ}K)\ln K_2^*$$

where sillimanite is the aluminum silicate of interest. Although $\Delta\overline{V}$, the change in partial molar volume for the reaction, is a constant for the end-member reaction (1.3045; Helgeson et al., 1978), Newton et al. (1977) and Cressey et al. (1978) found that pyrope–grossular and almandine–grossular solid solutions show significant excess partial molar volumes when the grossular component constitutes less than 40 mole percent of the solution. Thus, $\Delta\overline{V}$ for Equilibrium 2* will vary depending on the composition of the garnet in question. Newton and Haselton (1981) presented an analytical expression for calculating the partial molar volume of the grossular component in pyrope-grossular and almandine-grossular solutions, and we follow their method here. It should be noted that the effect of Mn on the partial molar volume of the grossular component is not accounted for in these equations. The equilibrium coefficient for reaction (2*) is given by:

$$K_2^* = \frac{(a_{an})^3}{(a_{gr})^3}$$

Following Ganguly and Kennedy (1974) and assuming Margules parameters from Table 7, the activity of the grossular component in garnet is computed as

$$a_{gr} = (X_{gr})\exp$$

$$\frac{[3300 - 1.5(T)](X_{py}^2 + X_{al}X_{py} + X_{py}X_{sp})}{RT} \quad (10)$$

Table 8. Temperatures calculated from Equilibrium 1* for $P = 3760$ bars using various values of W_{MgMn}

SAMPLE#	Values of W_{MgMn}
	3500	3000	2000	1000	0
78B	544°C	540	518	497	477
80D	583	573	554	536	518
90A	598	582	552	524	498
92D	578	566	543	521	500
145E	598	584	557	531	507
146B	670	649	609	572	538
146D	603	583	546	512	481

Obtaining a useful expression for the activity of anorthite in plagioclase is more difficult. Orville (1972) found $\gamma_{an} = 1.276$ at 700°C and 2 kbar for the compositional range of interest, but is unclear how to extrapolate this value to lower temperatures and higher pressures. Based on high-temperature calorimetry studies, Newton et al. (1980) suggest that:

$$RT\ln\gamma_{an} = X_{ab}^2[W_{Ca} + 2X_{an}(W_{Na} - W_{Ca})] \qquad (11)$$

where $W_{Ca} = 2025$ cal/mol and $W_{Na} = 6746$ cal/mol. Kerrick and Darken (1975) presented a variety of simple models based on statistical mechanics that could be used to account for the configurational entropy of plagioclase mixing in activity calculations. Of these, Newton et al. (1980) suggest that the "Al-avoidance" model is most consistent with Orville's (1972) experimental data. That is:

$$a_{an} = \gamma_{an} \cdot \frac{X_{an}(1 + X_{an})^2}{4} \qquad (12)$$

We have applied the above equations—the Goldsmith (1980) experimental determination of the end member reaction as discussed by Newton and Haselton (1981) (Equation 2*), with corrections for a_{gr} (Equation 11) and a_{an} (Equation 12)—to the Mt. Moosilauke samples, assuming $T = 501$°C. The pressures calculated are generally *inconsistent* with Holdaway's (1971) estimate of 3760 bar for the triple point pressure (Table 9). Of all the possible sources of error, it seems most likely that this reflects problems in the activity–composition relationships assumed for plagioclase. As pointed out by Newton and Haselton (1981), Equation (12) is strictly valid only for the high structural state plagioclase for which the laboratory data of Orville (1972) and Newton et al., (1980) were obtained. Al-

Si ordering at lower temperatures may invalidate this expression. Table 9 also shows pressures calculated for the Mt. Moosilauke samples using the activity coefficient formulation of Newton et al., (1980) and Kerrick and Darken's (1975) Model 4, which assumes complete local electrostatic neutrality and complete Al–Si ordering (i.e., $a_{an} = \gamma_{an}X_{an}$). In this case, pressures are unreasonably low and in some cases negative.

Given these results, it seems useful to invert the problem and attempt to constrain plagioclase activity–composition relationships using the Mt. Moosilauke data. For simplicity, we adopt Kerrick and Darken's Model 4 such that:

$$a_{an} = \gamma_{an} X_{an} \qquad (13)$$

Table 9 shows pressures calculated using values for γ_{an} of 1.276 (Orville's recommended value), 1.8 and 2.0. Results that are most consistent with Holdaway's triple point are obtained for $\gamma_{an} = 2.0$. Thus, we suggest that the expression presented by Newton et al., (1980) for γ_{an} may overcorrect for plagioclase non-ideality at ~500°C by a factor of two or more.

Discussion

Figure 7 illustrates $P–T$ estimates obtained for the Mt. Moosilauke samples as a result of simultaneous solution of Equilibria 1* and 2*. In generating this diagram, we have used the Ferry and Spear (1978) and Newton and Haselton (1981) equilibrium constant equations, and we calculated activities using Equations (9), (10), and (13) assuming Margules parameters from Table 7 and $\gamma_{an} = 2.0$. Estimates for each sample are in reasonably good agreement with those shown in Figure 6a, although there is somewhat less scatter in Figure 7. It should be stated explicitly that the tight cluster of points on this figure around Holdaway's triple point does not prove the "accuracy" of the calibrations used, since triple point $P–T$ conditions were assumed in their derivation. However, Figure 7 *does* show that calibrations of Equilibria 1 and 2 made using a consistent set of solution models for garnet and plagioclase can yield reasonable pressure and temperature estimates for amphibolite facies assemblages. Because of uncertainties in Margules parameters for garnet solid solutions (especially those involving manganese) and in activity–composition relationships for plagioclase, the general applicability of the calibrations presented here is unclear. We

Table 9. Calculated pressures from Equilibrium 2* for $T = 501$°C using different activity models for plagioclase

#	A	B	C	D	E
78B	5058	895	5533	4297	3918
80D	3654	457	5056	3822	3444
90A	5148	1137	5399	4176	3801
92D	4750	521	5147	3910	3493
145E	4751	317	4786	3546	3167
146B	3163	−253	4319	3096	2722
146D	3093	−290	4274	3052	2677

A) γ_{an} from Newton et al. (1980) with Al-avoidance model.
B) γ_{an} from Newton et al. (1980) with Al-Si ordering and local charge balance.
C) $\gamma_{an} = 1.276$ with Al-Si ordering and local charge balance.
D) $\gamma_{an} = 1.8$ with Al-Si ordering and local charge balance.
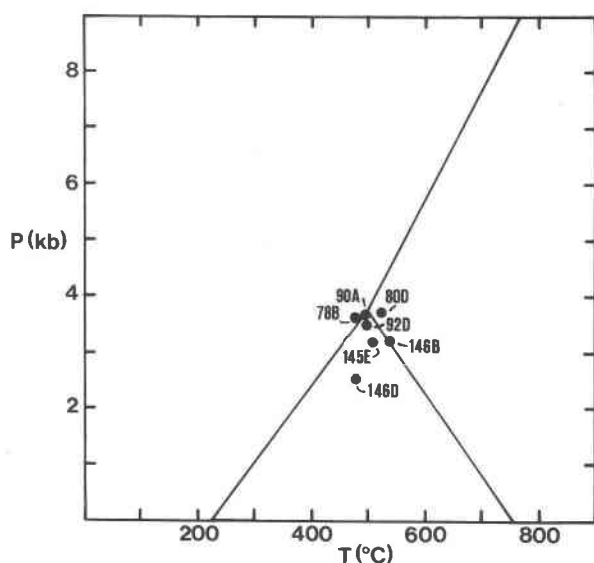E) $\gamma_{an} = 2.0$ with Al-Si ordering and local charge balance.

Fig. 7. *P–T* diagram showing the results of simultaneous solution of equilibria 1* and 2* for all samples. Aluminosilicate stability fields after Holdaway (1971) are shown for reference.

suggest discretion in their use for samples that crystallized under granulite facies conditions (where the Newton *et al.*, 1980, γ_{an} expression may be more appropriate than our value of $\gamma_{an} = 2.0$), and for samples containing high-Ti biotites and/or spessartine-rich garnets ($X_{sp} \geqslant 0.2$).

Throughout this paper, we have estimated errors in *P–T* estimates by propagation of assumed analytical errors through appropriate error magnification equations. This is certainly overly optimistic. Uncertainties in activity–composition relationships as well as in experimental determinations of end-member reactions compound the errors. Although it is difficult to quantify these effects, it seems likely that the maximum realistic precision of pressures and temperatures calculated from Equilibria 1 and 2 are on the order of ±1500 bar and ±50°C although the internal consistency of calculated *P*'s and *T*'s in "well-behaved" samples is approximately one-half to one-third this value (*e.g.*, Fig. 6A). Because of the empirical methods used for calibration of Equilibria 3 and 4, uncertainties involved in their use are certainly larger than these values.

Finally, despite our conclusion that Equilibria 1 and 2 accurately record peak metamorphic conditions at Mt. Moosilauke, the reliability of their doing so in rocks crystallized under all metamorphic conditions is suspect. Regardless of the quality of calibration of a geothermometer or geobarometer, retrograde reequilibration of a given petrologic

system during uplift and cooling of a metamorphic terrain can lead to significant underestimates of peak metamorphic conditions. In many cases, there is petrographic evidence for such back-reactions. However, operation of an exchange reaction such as Equilibrium 1 in a retrograde sense leaves no textural evidence, although it may be reflected in the compositional profiles of reequilibrated garnets (*e.g.*, Lasaga *et al.*, 1977). Since the retrograde operation of simple exchange reactions is probably a diffusional process and thus dependent on both absolute temperature and cooling rate, any exchange geothermometer or geobarometer should be used with caution in high-grade, slowly cooled, regional metamorphic terrains.

Conclusions

Temperatures and pressures recorded by fluid-independent geothermometers and geobarometers in pelites from the Mt. Moosilauke area, New Hampshire, are in very good agreement with *P–T* conditions predicted by the aluminum silicate triple point of Holdaway (1971). In particular, the calibrations of Ferry and Spear (1978) and Ghent *et al.* (1979) for garnet–biotite and garnet–plagioclase–aluminum silicate–quartz, respectively, appear to be fundamentally correct, at least for the compositional ranges encountered. However, their application to natural systems is complicated by inconsistent assumptions of garnet solution behavior in the calibrations as originally published. Recalibrations of these equilibria using a consistent set of mixing models is straightforward but hampered by uncertainties in Margules parameters and activity coefficients for garnet and plagioclase solid solution. By assuming that the Mt. Moosilauke samples equilibrated at pressure and temperature conditions near those of Holdaway's (1971) triple point, we have used the data presented in this paper to constrain these unknowns. Reasonable *P–T* estimates can be obtained for the Mt. Moosilauke samples by assuming: (1) that the only significant deviation from ideality in garnet solid solutions occurs along the pyrope–grossular binary; and (2) that there is complete Al–Si ordering in plagioclase and $\gamma_{an} \sim 2.0$. The validity of these assumptions at *P–T* conditions greatly removed from the aluminum silicate triple point is presently unknown.

References

Althaus, E. (1969) Experimental evidence that reaction of kyanite to form sillimanite is at least bivariant. American Journal of Science, 267, 273–277.

Anderson, P. A. M., Newton, R. C., and Kleppa, O. J. (1977) The enthalpy change of the andalusite–sillimanite reaction and the Al_2SiO_5 diagram. American Journal of Science, 277, 585–593.

Billings, M. P. (1937) Regional metamorphism of the Littleton–Moosilauke area, New Hampshire, Geological Society of America Bulletin, 48, 463–566.

Burnham, C. W., Holloway, J. R. and Davis, N. F. (1969) Thermodynamic properties of water to 1000°C and 10,000 bars. Geological Society of America Special Paper 132.

Chatterjee, N. D. (1972) The upper stability limit of the assemblage paragonite + quartz and its natural occurrences. Contributions to Mineralogy and Petrology, 34, 288–303.

Chatterjee, N. D. and Froese, E. (1975) A thermodynamic study of the pseudobinary join muscovite–paragonite in the system $KAlSi_3O_8–NaAlSi_3O_8–Al_2O_3–SiO_2–H_2O$. American Mineralogist, 60, 985–993.

Cheney, J. T., and Guidotti, C. V. (1979) Muscovite + plagioclase equilibria in sillimanite + quartz bearing metapelites, Puzzle Mountain area, northwest Maine. American Journal of Science, 279, 411–434.

Cressey, G., Schmid, R. and Wood, B. J. (1978) Thermodynamic properties of almandine–grossular garnet solid solutions. Contributions to Mineralogy and Petrology, 67, 397–404.

Dallmeyer, R. D. (1974) The role of crystal structure in controlling the partitioning of Mg and Fe^{2+} between coexisting garnet and biotite. American Mineralogist, 59, 201–203.

Ferry, J. M. (1980) A comparative study of geothermometers and geobarometers in pelitic schists from south-central Maine. American Mineralogist, 65, 720–732.

Ferry, J. M. and Spear, F. S. (1978) Experimental calibration of the partitioning of Fe and Mg between biotite and garnet. Contributions to Mineralogy and Petrology, 66, 113–117.

Ganguly, J. and Kennedy, G. C. (1974) The energetics of natural garnet solid solution: I. Mixing of the aluminosilicate endmembers. Contributions to Mineralogy and Petrology, 48, 137–148.

Ghent, E. D. (1976) Plagioclase–garnet–Al_2SiO_5–quartz: a potential geobarometer–geothermometer. American Mineralogist, 61, 710–714.

Ghent, E. D., Robbins, D. B., and Stout, M. Z. (1979) Geothermometry, geobarometry, and fluid compositions of metamorphosed calc-silicates and pelites, Mica Creek, British Columbia. American Mineralogist, 64, 874–885.

Ghent, E. D. and Stout, M. Z. (1981) Geobarometry and geothermometry of plagioclase–biotite–garnet–muscovite assemblages. Contributions to Mineralogy and Petrology, 76, 92–97.

Goldman, D. S. and Albee, A. L. (1977) Correlation of Mg/Fe partitioning between garnet and biotite with O^{18}/O^{16} partitioning between quartz and magnetite. American Journal of Science, 277, 750–761.

Goldsmith, J. R. (1980) Melting and breakdown reactions of anorthite at high pressures and temperatures. American Mineralogist, 65, 272–284.

Helgeson, H. C., Delany, J. M., Nesbitt, H. W., and Bird, D. K. (1978) Summary and critique of the thermodynamic properties of rock forming minerals. American Journal of Science, 278-A.

Holdaway, M. J. (1971) Stability of andalusite and the aluminosilicate phase diagram. American Journal of Science, 271, 97–131.

Hutcheon, I. (1979) Sulfide–oxide–silicate equilibria; Snow Lake, Manitoba. American Journal of Science, 279, 643–665.

Kerrick, D. M. and Darken, L. S. (1975) Statistical thermodynamic models for ideal oxide and silicate solid solutions, with application to plagioclase. Geochimica et Cosmochimica Acta, 39, 1431–1442.

Lasaga, A. C., Richardson, S. M., and Holland, H. D. (1977) The mathematics of cation diffusion and exchange between silicate minerals during retrograde metamorphism. In S. K. Saxena and S. Bhattacharji, Eds., Energetics of Geological Processes, p. 354–387, Springer-Verlag, New York.

Mueller, R. F. (1972) Stability of biotite: A discussion. American Mineralogist, 57, 300–316.

Naylor, R. S. (1971) Acadian orogeny: an abrupt and brief event. Science, 172, 558–560.

Newton, R. C. and Haselton, H. T. (1981) Thermodynamics of the garnet–plagioclase–Al_2SiO_5–quartz geobarometer. In R. C. Newton, et al., Eds., Thermodynamics of Minerals and Melts, p. 131–147, Springer-Verlag, New York.

Newton, R. C., Charlu, T. V., and Kleppa, O. J. (1977) Thermochemistry of high pressure garnets and clinopyroxenes in the system $CaO–MgO–Al_2O_3–SiO_2$. Geochimica et Cosmochimica Acta, 41, 369–377.

Newton, R. C., Charlu, T. V., and Kleppa, O. J. (1980) Thermochemistry of the high structural state plagioclases. Geochimica et Cosmochimica Acta, 44, 933–941.

Ohmoto, H., and Kerrick, D. (1977) Devolatilization equilibria in graphitic systems. American Journal of Science, 277, 1013–1044.

Orville, P. M. (1972) Plagioclase cation exchange equilibria with aqueous chloride solution: results at 700°C and 2000 bars in the presence of quartz. American Journal of Science, 272, 234–272.

Richardson, S. W. (1968) Staurolite stability in part of the system Fe–Al–Si–O–H. Journal of Petrology, 9, 467–489.

Rumble, D., III (1973) Andalusite, kyanite, and sillimanite from the Mount Moosilauke region, New Hampshire. Geological Society of American Bulletin, 84, 2423–2430.

Rumble, D. III, Ferry, J. M., Hoering, T. C. and Boucot, A. J. (1982) Fluid flow during metamorphism at the Beaver Brook fossil locality, New Hampshire. American Journal of Science, 282, 886–919.

Smith, F. G. (1966) Geological data processing using Fortran IV. Harper & Row, New York.

Spear, F. S. (1980) Plotting stereoscopic phase diagrams. American Mineralogist, 65, 1291–1293.

Strens, R. G. J. (1968) Stability of Al_2SiO_5 solid solutions. Mineralogical Magazine, 36, 839–849.

Thompson, A. B. (1976) Mineral reactions in pelitic rocks: II. Calculation of some P–T–X (Fe–Mg) phase relations. American Journal of Science, 276, 401–454.

Thompson, J. B., Jr. (1957) The graphical analysis of mineral assemblages in pelitic schists. American Mineralogist, 42, 842–858.

Thompson, J. B., Jr., and Norton, S. A. (1968) Paleozoic regional metamorphism in New England and adjacent areas. In E-an Zen *et al.*, Eds., Studies of Appalachian geology, p. 319–327. John Wiley, New York.

Zen, E-an (1969) The stability relations of the polymorphs of aluminum silicate: a survey and some comments. American Journal of Science, 267, 293–309.